Discrete Poincaré Duality Angles as Shape Signatures on Simplicial Surfaces with Boundary

Konstantin Poelke and Konrad Polthier

Abstract We introduce and explore the concept of *discrete Poincaré duality angles* as an intrinsic measure that quantifies the metric-topological influence of boundary components to compact surfaces with boundary. Based on a discrete Hodge-Morrey-Friedrichs decomposition for piecewise constant vector fields on simplicial surfaces with boundary, the discrete Poincaré duality angles reflect a deep linkage between metric properties of the spaces of discrete harmonic Dirichlet and Neumann fields and the topology of the underlying surface, and may act as a new kind of shape signature. We provide an algorithm for the computation of these angles and discuss them on several exemplary surface models.

1 Introduction

Hodge-type decomposition statements form an indispensable tool for the analysis and structural understanding of vector fields and more generally differential forms on manifolds. Dating back at least to Helmholtz' classical result [18] on the decomposition of a vector field into a divergence-free and a rotation-free component, there has been a remarkable evolution of extensions and generalizations. Nowadays there is a well-developed theory for Hodge decompositions of differential forms of Sobolev class (see [15] for an overview), which is of central importance e.g. for finite element Galerkin methods for problems involving vector fields such as Maxwell's equations or Navier-Stokes systems. A surprising property is the strong linkage of certain spaces of harmonic forms to the topology of the underlying manifold, whose first encounter is given by de Rham's theorem, stating that on a closed oriented Riemannian manifold the space of harmonic k-forms is isomorphic to the k-th cohomology with real coefficients. On a surface with non-empty boundary, the corresponding statement applies to the spaces of harmonic Dirichlet fields $\mathscr{H}^1_D$

K. Poelke (✉) · K. Polthier
Freie Universität Berlin, Berlin, Germany
e-mail: konstantin.poelke@fu-berlin.de; konrad.polthier@fu-berlin.de

H. Carr et al. (eds.), *Topological Methods in Data Analysis and Visualization V*,
Mathematics and Visualization, https://doi.org/10.1007/978-3-030-43036-8_16

and Neumann fields $\mathscr{H}^1_N$, which are subspaces of all harmonic fields with certain boundary conditions imposed. However, there are now two decompositions—one including $\mathscr{H}^1_D$, the other one including $\mathscr{H}^1_N$—and in general there is no single L^2-orthogonal decomposition including both these spaces at the same time. A recent result by Shonkwiler [16, 17] identifies the reason for this non-orthogonality as the existence of non-empty subspaces representing the *interior cohomology* of the manifold (in contrast to the *cohomology induced by the boundary components*), which establishes another astonishing linkage between metric properties and the topology. In particular, the principal angles between $\mathscr{H}^1_N$ and $\mathscr{H}^1_D$ seem to act as an indicator for the influence of boundary components on the overall geometry and therefore as a theoretical shape signature.

Contributions The main contribution of this article is the introduction of discrete Poincaré duality angles in Sect. 4, based on a discretization of harmonic Neumann and Dirichlet fields by piecewise constant vector fields on simplicial surfaces with boundary. Furthermore, we provide an algorithm for their numerical computation, using a singular value decomposition of a matrix whose size only depends on the topological complexity of the surface. Finally, we compute these angles for a few exemplary models and discuss their interpretation as shape signatures.

Related Work The literature on Hodge-type decomposition statements is vast and has a long history. For a modern treatment and a good overview on smooth and Sobolev-class Hodge-type decomposition statements see [15] and the literature referenced therein. The recent work by Shonkwiler [16, 17] introduces the concept of Poincaré duality angles and the splitting of Neumann and Dirichlet fields into interior cohomology- and boundary cohomology-representing subspaces on smooth oriented Riemannian manifolds. A general background on differential forms, Hodge decompositions and homology theory of manifolds can be found in standard textbooks such as [5, 9] and [10].

For the numerical treatment of vector fields there is a variety of discretization strategies available, cf. the overview article [3]. For instance, the *finite element exterior calculus* [2] by Arnold et al. introduces families of spaces of polynomial differential forms of arbitrary degree and generalizes classical ansatz spaces such as the Raviart-Thomas elements or Nédélec's elements. The *discrete exterior calculus* [7] by Hirani defines discrete differential forms as synonyms for simplicial cochains and relies on a dual grid to derive metric-dependent properties. Here we focus on a discretization by *piecewise constant vector fields* (PCVFs). Their usage and analysis in geometry processing tasks goes back at least to the work by Polthier and Preuss [13] and Wardetzky [19]. The interplay of linear Lagrange and Crouzeix-Raviart elements as ansatz spaces for gradients and cogradients which is central to these works can already be found in [1] for the special case of a simply-connected domain in $\mathbb{R}^2$. Since then, PCVFs have become a main ingredient for frame field modelling [20], remeshing [6, 14] or surface parameterization [8], just to name a few examples.

A complete, structurally consistent set of Hodge-type decompositions for PCVFs on simplicial surfaces and solids with boundary has been recently developed by

Poelke and Polthier [11, 12], and we refer the reader to these works for all details concerning theory, discretization, implementation and numerical solving left out in this article.

Outline Section 2 reviews the necessary background of smooth Hodge-type decompositions and Poincaré duality angles on smooth manifolds. In Sect. 3 we state the most important results from a discretization by piecewise constant vector fields as developed in [11, 12]. Furthermore, some exemplary angles between discrete harmonic Neumann and Dirichlet fields are computed, serving as a motivation for the introduction of discrete Poincaré duality angles, which are then introduced, computed and discussed in Sect. 4.

2 Hodge-Type Decompositions, Topology and Duality Angles

In its modern formulation, the Hodge decomposition theorem states that on a closed oriented Riemannian manifold M the space Ω^k of smooth k-forms can be decomposed L^2-orthogonally as

$$\Omega^k = \mathrm{d}\Omega^{k-1} \oplus \delta\Omega^{k+1} \oplus \mathscr{H}^k \tag{1}$$

where $\mathscr{H}^k$ is the space of harmonic k-forms satisfying $\mathrm{d}\omega = \delta\omega = 0$. Here and in the following, $\oplus$ always denotes an L^2-orthogonal direct sum. A remarkable result is de Rham's theorem which provides an isomorphism $\mathscr{H}^k \cong H^k(M)$ between the space of harmonic k-forms and the k-th cohomology with real coefficients on M, and therefore identifies the dimension of $\mathscr{H}^k$ as a *topological* invariant.

As soon as the manifold M has a non-empty boundary $\partial M \neq \emptyset$, Eq. (1) is no longer valid. Instead, the analogous splitting is now given by *two* decomposition statements known as the *Hodge-Morrey-Friedrichs decomposition* (see [15]):

$$\begin{aligned}\Omega^k &= \mathrm{d}\Omega_D^{k-1} \oplus \delta\Omega_N^{k+1} \oplus (\mathscr{H}^k \cap \mathrm{d}\Omega^{k-1}) \oplus \mathscr{H}_N^k \\ &= \mathrm{d}\Omega_D^{k-1} \oplus \delta\Omega_N^{k+1} \oplus (\mathscr{H}^k \cap \delta\Omega^{k+1}) \oplus \mathscr{H}_D^k.\end{aligned}$$

Here, the subscript $_D$ denotes *Dirichlet boundary conditions* (i.e. the tangential part $\mathbf{t}(\omega)$ of a differential form ω has to vanish along ∂M) and $_N$ denotes *Neumann boundary conditions* (i.e. the normal part $\omega\,|_{\partial M} - \mathbf{t}(\omega)$ has to vanish along ∂M) which are imposed on the corresponding spaces. Again, there are isomorphisms $\mathscr{H}_N^k \cong H^k(M)$ and $\mathscr{H}_D^k \cong H^k(M, \partial M)$, respectively, with the latter space $H^k(M, \partial M)$ denoting the k-th *relative* cohomology of M.

With respect to the characterization of vector fields on surfaces with boundary, a natural question is whether there is a single orthogonal decomposition including $\mathscr{H}_N^1$ and $\mathscr{H}_D^1$ at the same time. To this end, we say that a surface M *is of type*

$\Sigma_{g,m}$, if M is a compact orientable surface of genus $g \geq 0$ with $m \geq 0$ boundary components. We have the following result [11, Lemma 2.4.5]:

Lemma 1 *Let M be a surface of type $\Sigma_{0,m}$. Then there is an L^2-orthogonal decomposition*

$$\Omega^1 = \mathrm{d}\Omega^0_D \oplus \delta\Omega^2_N \oplus (\mathrm{d}\Omega^0 \cap \delta\Omega^2) \oplus \mathscr{H}^1_D \oplus \mathscr{H}^1_N.$$

Lemma 1 includes the common case of two-dimensional flat domains embedded in $\mathbb{R}^2$. On the other hand, if $g \geq 1$ the sum $\mathscr{H}^1_D \oplus \mathscr{H}^1_N$ is not L^2-orthogonal any more. A recent result by Shonkwiler [16, 17] identifies subspaces of $\mathscr{H}^1_D$ and $\mathscr{H}^1_N$, or more generally $\mathscr{H}^k_D$ and $\mathscr{H}^k_N$, representing the cohomology corresponding to the *inner topology* of M as the reason for this non-orthogonality. Shonkwiler introduces the spaces

$$\begin{aligned}
\mathscr{H}^k_{N,\mathrm{co}} &:= \mathscr{H}^k_N \cap \delta\Omega^{k+1} \\
\mathscr{H}^k_{N,\partial\mathrm{ex}} &:= \{\omega \in \mathscr{H}^k_N : \iota^*\omega \in \mathrm{d}\Omega^{k-1}(\partial M)\} \\
\mathscr{H}^k_{D,\mathrm{ex}} &:= \mathscr{H}^k_D \cap \mathrm{d}\Omega^{k-1} = \star\mathscr{H}^{n-k}_{N,\mathrm{co}} \\
\mathscr{H}^k_{D,\partial\mathrm{co}} &:= \{\omega \in \mathscr{H}^k_D : \iota^*(\star\omega) \in \mathrm{d}\Omega^{n-k-1}(\partial M)\} = \star\mathscr{H}^{n-k}_{N,\partial\mathrm{ex}}
\end{aligned} \tag{2}$$

of *coexact Neumann*, *boundary-exact Neumann*, *exact Dirichlet* and *boundary-coexact Dirichlet k-forms*, respectively. Here, $\iota : \partial M \hookrightarrow M$ denotes the inclusion, $\star$ is the Hodge star and n is the dimension of M. It is then shown [16, Thm. 2.1.3] that always $\mathscr{H}^k_{D,\mathrm{ex}} \perp \mathscr{H}^k_N$ and $\mathscr{H}^k_{N,\mathrm{co}} \perp \mathscr{H}^k_D$, but in general $\mathscr{H}^k_{N,\partial\mathrm{ex}} \not\perp \mathscr{H}^k_{D,\partial\mathrm{co}}$. Furthermore, the subspaces $\mathscr{H}^k_{D,\mathrm{ex}}$ and $\mathscr{H}^k_{N,\mathrm{co}}$ can be directly related to cohomology information that is induced by the boundary components, whereas the critical subspaces $\mathscr{H}^k_{N,\partial\mathrm{ex}}$ and $\mathscr{H}^k_{D,\partial\mathrm{co}}$ are related to the "interior topology" of the manifold, and it is this presence of interior topology that causes the orthogonality to fail. The amount of failure can be measured by the *Poincaré duality angles*, which are the principal angles between $\mathscr{H}^k_D$ and $\mathscr{H}^k_N$. Since the boundary-representing subspaces are always orthogonal, the interesting, non-trivial principal angles therefore arise between the spaces $\mathscr{H}^k_{N,\partial\mathrm{ex}}$ and $\mathscr{H}^k_{D,\partial\mathrm{co}}$. Shonkwiler computes these angles analytically for the complex projective space with an open ball removed, and the Grassmannian with a tubular neighbourhood of a sub-Grassmannian removed [16, Chap. 3 & 4]. In both cases the Poincaré duality angles quantify how far the manifolds are from being closed. In particular, shrinking the size of the boundary component lets the angles tend to zero, whereas increasing the size lets them tend to $\pi/2$. Furthermore, the order of convergence seems to encode the codimension of the removed submanifold, which is posed as a conjecture [16, Conj. 3]. For general manifolds, though, the analytic computation of these angles seems difficult or even intractable.

3 Discrete Neumann and Dirichlet Fields

Now, let $M_h \subset \mathbb{R}^3$ be a compact, orientable simplicial surface with (possibly empty) boundary, triangulated by affine triangles, equipped with the locally Euclidean metric. We use the subscript h to distinguish between the simplicial surface and discrete function spaces, and their smooth counterparts. It can be thought of as a discretization parameter and commonly refers to the maximum diameter of the affine triangles in the triangulation of M_h.

Let $\mathscr{X}_h$ denote the space of PCVFs on M_h, which are given by one tangent vector X_T per affine triangle T of M_h, and let $\mathscr{L}$ and $\mathscr{F}$ denote the finite element spaces of linear Lagrange and Crouzeix-Raviart elements on M_h. To be precise, $\mathscr{L}$ denotes the space of all continuous functions on M_h that are linear when restricted to an individual triangle T, and $\mathscr{F}$ is the space of all L^2-functions on M_h that are represented by a linear function when restricted to an individual triangle T such that the values of these linear representatives agree at the edge midpoint between any two adjacent triangles. Therefore, an element in $\mathscr{L}$ is uniquely defined by its values at vertices, whereas an element in $\mathscr{F}$ is uniquely defined by its values at edge midpoints. We denote by $\mathscr{L}_0 \subset \mathscr{L}$ the subspace of all linear Lagrange functions that vanish at the boundary, and by $\mathscr{F}_0 \subset \mathscr{F}$ the subspace of all Crouzeix-Raviart functions that vanish at all midpoints of boundary edges. Furthermore, we denote by

$$\begin{aligned} \nabla\mathscr{L} &:= \{\nabla\varphi : \varphi \in \mathscr{L}\} & \nabla\mathscr{L}_0 &:= \{\nabla\varphi : \varphi \in \mathscr{L}_0\} \\ J\nabla\mathscr{F} &:= \{J\nabla\psi : \psi \in \mathscr{F}\} & J\nabla\mathscr{F}_0 &:= \{J\nabla\psi : \psi \in \mathscr{F}_0\}, \end{aligned}$$

the gradient and cogradient spaces, respectively, formed by these ansatz functions. Here, ∇ is the element-wise surface gradient and J denotes a counter-clockwise (with respect to a fixed unit normal field) rotation by $\pi/2$ in the tangent plane of each triangle. In other words, if X_T is a vector in the tangent plane of a triangle T, and N_T is a unit normal on T, then $JX_T := N_T \times X_T$ acts as the cross-product with N_T.

It is not hard to prove that the spaces $\nabla\mathscr{L}_0$ and $J\nabla\mathscr{F}_0$ are L^2-orthogonal to each other [12, Sec. 3.1], even if $\partial M_h = \emptyset$ in which case we have $\mathscr{L}_0 = \mathscr{L}$ and $\mathscr{F}_0 = \mathscr{F}$. Let $\mathscr{H}_h$ denote the space of *discrete harmonic PCVFs*, defined as the L^2-orthogonal complement of the sum $\nabla\mathscr{L}_0 \oplus J\nabla\mathscr{F}_0$. If $\partial M_h = \emptyset$, i.e. if M_h is a closed surface of genus g, then there is a single, orthogonal decomposition of the space of PCVFs, given by

$$\mathscr{X}_h = \nabla\mathscr{L} \oplus J\nabla\mathscr{F} \oplus \mathscr{H}_h \tag{3}$$

and furthermore dim $\mathscr{H}_h = 2g$ [19, Thm. 2.5.2]. On the other hand, if $\partial M_h \neq \emptyset$, i.e. $m \geq 1$, there are now two discrete Hodge-Morrey-Friedrichs decompositions [12, Cor. 3.3]:

Definition and Lemma 2 *If $M_h \neq \emptyset$, there are two L^2-orthogonal decompositions*

$$\mathscr{X}_h = \nabla\mathscr{L}_0 \oplus J\nabla\mathscr{F}_0 \oplus (\mathscr{H}_h \cap \nabla\mathscr{L}) \oplus \mathscr{H}_{h,N} \tag{4}$$

$$= \nabla\mathscr{L}_0 \oplus J\nabla\mathscr{F}_0 \oplus (\mathscr{H}_h \cap J\nabla\mathscr{F}) \oplus \mathscr{H}_{h,D} \tag{5}$$

where $\mathscr{H}_{h,N}$ and $\mathscr{H}_{h,D}$ are the spaces of discrete Neumann and Dirichlet fields, *defined as the L^2-orthogonal complement of the sum of the first three subspaces in Eqs.* (4) *and* (5)*, respectively.*

Furthermore, we have discrete de Rham isomorphisms $\mathscr{H}_{h,N} \cong H^1(M_h)$ and $\mathscr{H}_{h,D} \cong H^1(M_h, \partial M_h)$, and by Poincaré-Lefschetz duality it follows dim $\mathscr{H}_{h,D} =$ dim $\mathscr{H}_{h,N} = 2g + m - 1$ for a surface of type $\Sigma_{g,m}$ with $m \geq 1$. Bases for the spaces $\mathscr{H}_{h,N}$ and $\mathscr{H}_{h,D}$ are shown in Fig. 1 for a surface of type $\Sigma_{0,3}$ and in Fig. 2 on a hand model with four boundary components, which is of type $\Sigma_{1,4}$.

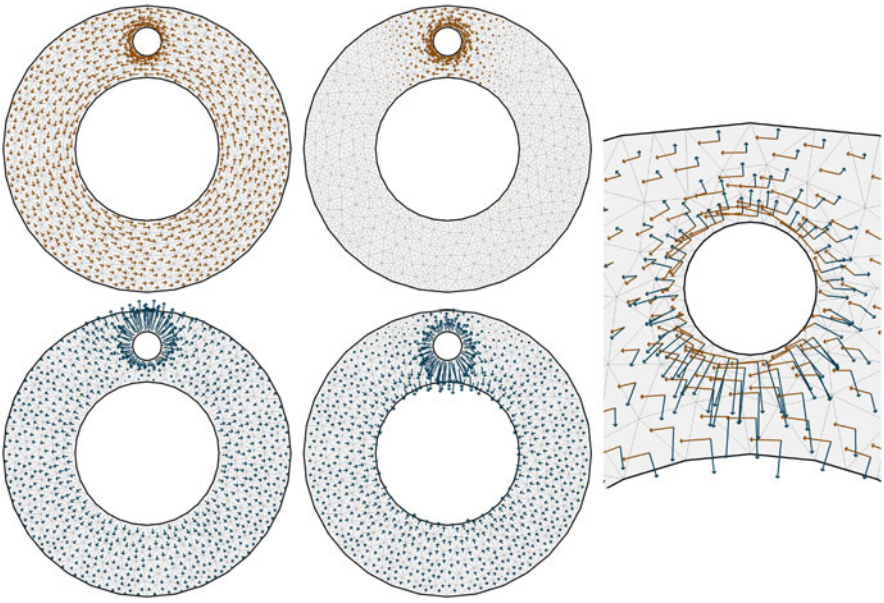

Fig. 1 Basis fields $X_{N,1}, X_{N,2}$ for $\mathscr{H}_{h,N}$ (top row) and $X_{D,1}, X_{D,2}$ for $\mathscr{H}_{h,D}$ (bottom row) on an annulus with a hole ("AwH"), which is a surface of type $\Sigma_{0,3}$. As in the smooth case, discrete Dirichlet fields are characterized by having a vanishing tangential component along the boundary, whereas discrete Neumann fields have an almost vanishing normal component (for details on why the normal component is not necessarily strictly vanishing in this discretization, see [12, Section 3.1]). Each discrete Neumann field is L^2-orthogonal to each discrete Dirichlet field on this model. Locally, though, these fields need not be orthogonal, as can be seen in the rightmost image, where $X_{N,1}$ and $X_{D,2}$ are shown in a close-up

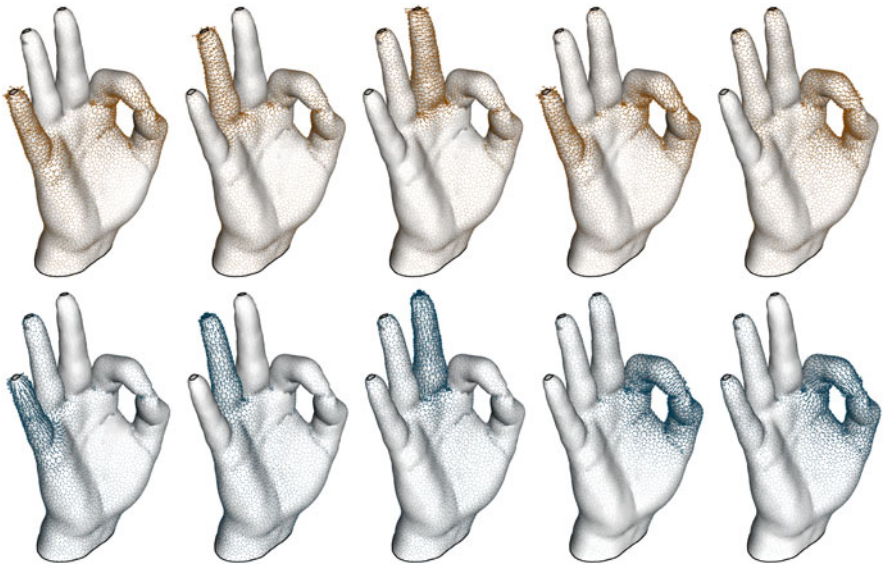

Fig. 2 Bases for the spaces $\mathscr{H}_{h,N}$ (top row) and $\mathscr{H}_{h,D}$ (bottom row) on a hand model with four boundary components (one hole cut out at each finger tip and the fourth one at the wrist)

Table 1 Angles between the basis fields for $\mathscr{H}_{h,N}$ and $\mathscr{H}_{h,D}$ on the flat AwH-model from Fig. 1 and the TwC-model from Fig. 3 in radians. The bold values in the TwC table belong to the two pairs in the close-up Fig. 4

AwH	$X_{D,1}$	$X_{D,2}$
$X_{N,1}$	1.57	1.57
$X_{N,2}$	1.57	1.57

TwC	$X_{D,1}$	$X_{D,2}$	$X_{D,3}$
$X_{N,1}$	2.30	1.57	**0.74**
$X_{N,2}$	1.62	1.57	1.55
$X_{N,3}$	2.41	1.58	**2.31**

As in the smooth case in Lemma 1, for simplicial surfaces of type $\Sigma_{0,m}$ both spaces are always L^2-orthogonal to each other and consequently there is a single complete discrete decomposition [12, Lemma 3.10]

$$\mathscr{X}_h = \nabla\mathscr{L}_0 \oplus J\nabla\mathscr{F}_0 \oplus (J\nabla\mathscr{F} \cap \nabla\mathscr{L}) \oplus \mathscr{H}_{h,D} \oplus \mathscr{H}_{h,N}. \tag{6}$$

The numerical angles in Table 1 confirm this result for the surface of type $\Sigma_{0,3}$ from Fig. 1. Each angle $\alpha = \measuredangle(X, Y)$ is computed as usual by

$$\cos\alpha = \frac{\langle X, Y\rangle_{L^2}}{\|X\|_{L^2}\,\|Y\|_{L^2}} \quad \text{for} \quad X \in \mathscr{H}_{h,N},\ Y \in \mathscr{H}_{h,D}.$$

Note that the orthogonality of the shown vector fields is always meant with respect to the L^2-product on $\mathscr{X}_h$. Locally, these fields are in general not orthogonal, see the rightmost image in Fig. 1.

In contrast, the example in Fig. 3 shows bases for the three-dimensional spaces $\mathscr{H}_{h,N}$ and $\mathscr{H}_{h,D}$ on a torus with a cylinder attached, which is of type $\Sigma_{1,2}$. Whereas both the second Neumann and Dirichlet fields form an angle of almost $\pi/2$ to all other fields, this is not true for the those fields, whose masses concentrate on the toroidal region. Figure 4 shows a close-up of two pairs of fields on the toroidal region, one forming locally acute angles, the other forming locally obtuse angles. As their mass on the cylindrical region is negligible, the local situation here dominates the L^2-angle, and indeed the first pairing forms an acute L^2-angle of 0.74 radians,

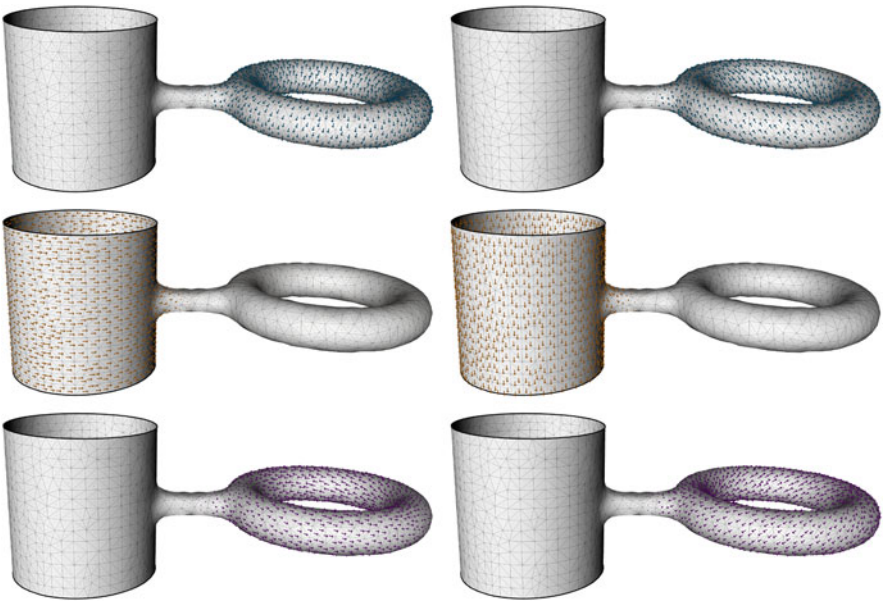

Fig. 3 Basis fields $X_{N,1}$, $X_{N,2}$, $X_{N,3}$ for $\mathscr{H}_{h,N}$ (left column, top to bottom) and $X_{D,1}$, $X_{D,2}$, $X_{D,3}$ for $\mathscr{H}_{h,D}$ (right column, top to bottom) on a torus with a cylinder attached ("TwC"), which is topologically a surface of type $\Sigma_{1,2}$. The fields in the first and third row all concentrate their mass in the same fashion along the longitudinal and latitudinal cycles that reflect homology generated by the torus

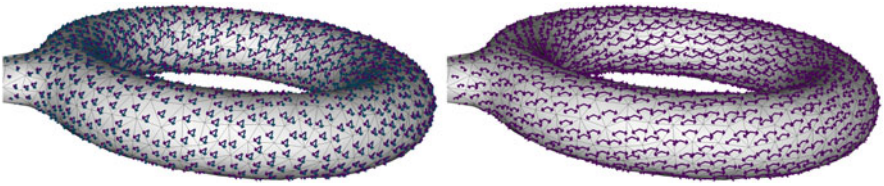

Fig. 4 Two pairings of Neumann and Dirichlet fields from the bases shown in Fig. 3. The left image shows the first Neumann field $X_{N,1}$ and the third Dirichlet field $X_{D,3}$, forming locally acute angles on each triangle on the torus region. The right image shows the third Neumann field $X_{N,3}$ and the third Dirichlet field $X_{D,3}$, forming obtuse angles

whereas the second pairing forms an obtuse L^2-angle of 2.31 radians, see Table 1. Consequently, the spaces $\mathscr{H}_{h,N}$ and $\mathscr{H}_{h,D}$ cannot appear simultaneously in a single orthogonal decomposition on this model.

4 Discrete Poincaré Duality Angles as Shape Signatures

The previous examples depend on the particular choice of basis vector fields whose pairwise angles are measured. In order to get rid of this dependence, we consider instead the principal angles between the vector spaces $\mathscr{H}_{h,N}$ and $\mathscr{H}_{h,D}$, which are independent of any concrete choice of basis. In accordance with the smooth situation we call these principal angles *discrete Poincaré duality angles* and define them as follows:

Definition 3 (Discrete Poincaré Duality Angles) The *discrete Poincaré duality angles* on M_h are the principal angles $0 \leq \theta_1 \leq \theta_2 \leq \cdots \leq \theta_{2g+m-1} \leq \pi/2$ between the spaces $\mathscr{H}_{h,N}$ and $\mathscr{H}_{h,D}$, defined recursively by

$$\theta_1 := \measuredangle(u_1, v_1) := \min\{\measuredangle(u, v) : u \in \mathscr{H}_{h,N}, v \in \mathscr{H}_{h,D}\}$$

$$\theta_k := \measuredangle(u_k, v_k) := \min\left\{\measuredangle(u, v) : \begin{array}{l} u \in \mathscr{H}_{h,N}, v \in \mathscr{H}_{h,D} \text{ with } u \perp u_i, v \perp v_i \\ \text{for all } i = 1, \ldots, k-1 \end{array}\right\}.$$

We stress again that the sequence of discrete Poincaré duality angles, being defined as principal angles between linear subspaces of $\mathscr{X}_h$, only depends on $\mathscr{H}_{h,N}$ and $\mathscr{H}_{h,D}$, but not on a concrete choice of vectors. In particular, whereas the sequence $\theta_1, \theta_2, \ldots$ is uniquely determined for a given simplicial surface M_h, the vectors u_k, v_k realizing an angle θ_k are not (cf. [4]).

A trivial consequence of Definition 3 is that if $\theta_i = \pi/2$ for all i, then clearly $\mathscr{H}_{h,N} \perp \mathscr{H}_{h,D}$. In general, though, these angles measure the deviation of the spaces $\mathscr{H}_{h,N}$ and $\mathscr{H}_{h,D}$ from being orthogonal to each other. In this sense they can be thought of as a quantitative value that measures how far away the two discrete Hodge-Morrey-Friedrichs-decompositions Eqs. (4) and (5) are from being either the single decomposition Eq. (1) on a closed surface of type $\Sigma_{g,0}$ or the complete orthogonal decomposition Eq. (6) on a domain coming from a sphere, i.e. a surface of type $\Sigma_{0,m}$.

This is illustrated by the sequence in Fig. 5, which shows a torus surface of type $\Sigma_{1,2}$. In the beginning the boundary components are almost negligible and start to grow until the final surface in the sequence is ultimately dominated by the boundary components. This behaviour is numerically reflected by the sequence of the corresponding Poincaré duality angles given in Table 2.

Figure 6 shows a similar sequence of a genus-2-surface with three boundary components, so it is of type $\Sigma_{2,3}$. Here, the leftmost growing boundary component has a dramatic influence on the pair (θ_3, θ_4), corresponding to the left torus region. The other duality angles remain mostly unaffected.

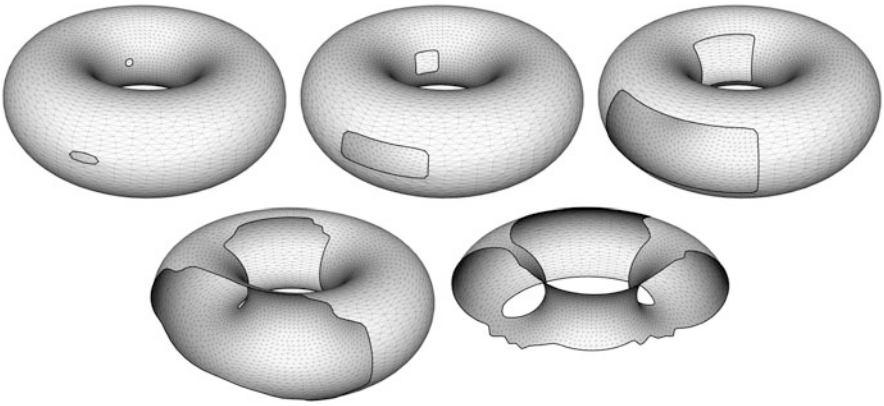

Fig. 5 A torus sequence (denoted "g1h2(a) – g1h2(e)") with two growing boundary components. Although all five models are topologically equivalent, the influence of the boundary components is drastically increasing and turns the initially almost closed surface into a surface dominated by its boundary. This is reflected by the numerical values in Table 2

Table 2 Poincaré duality angles for all experiments

Model	Type	θ_1	θ_2	θ_3	θ_4	θ_5	θ_6
TwC	$\Sigma_{1,2}$	$1.73 \cdot 10^{-4}$	$1.76 \cdot 10^{-4}$	1.57	–	–	–
Hand	$\Sigma_{1,4}$	0.03	0.03	1.57	1.57	1.57	–
g1h2(a)	$\Sigma_{1,2}$	0.08	0.09	1.57	–	–	–
g1h2(b)	$\Sigma_{1,2}$	0.28	0.28	1.57	–	–	–
g1h2(c)	$\Sigma_{1,2}$	0.62	0.62	1.57	–	–	–
g1h2(d)	$\Sigma_{1,2}$	0.95	0.95	1.57	–	–	–
g1h2(e)	$\Sigma_{1,2}$	1.32	1.32	1.57	–	–	–
g2h3(a)	$\Sigma_{2,3}$	0.13	0.14	0.26	0.27	1.57	1.57
g2h3(b)	$\Sigma_{2,3}$	0.14	0.15	0.70	0.70	1.57	1.57
g2h3(c)	$\Sigma_{2,3}$	0.21	0.21	1.14	1.14	1.57	1.57

A dash means that these angles do not exist for the respective surface, as there are always only $2g + m - 1$ duality angles

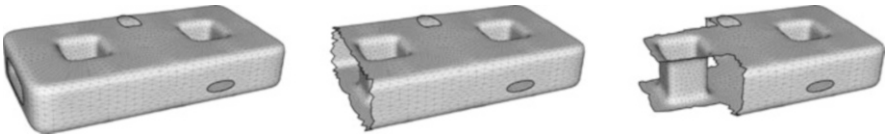

Fig. 6 A sequence of a surface (denoted "g2h3(a) – g2h3(c)") of type $\Sigma_{2,3}$. The leftmost boundary is growing and dominates the left torus component. This is reflected by the increasing angles θ_3 and θ_4 in Table 2, corresponding to the left toroidal region. Note that the other toroidal region remains mostly unaffected by the growing boundary component—the angles θ_1 and θ_2 merely increase from 0.13 to 0.21

The small angles θ_1 and θ_2 on the TwC-model suggest that the torus region is almost decoupled from the boundary components, and indeed this was the intention behind this rather artificial model. Here, $\mathscr{H}_{h,N}$ and $\mathscr{H}_{h,D}$ almost collapse to a single harmonic space of dimension 2 which would exist on a perfect torus. Moreover, by comparing with the values in Table 1 we see that the vector fields $X_{N,1}$, $X_{N,3}$ and $X_{D,1}$, $X_{D,3}$ in Fig. 3 are far from realizing the discrete Poincaré duality angles.

To a lesser extent, this situation is also prevalent for the hand model, where the torus region formed by thumb and index finger appears more integrated in the remaining part of the surface. Consequently, the angles θ_1 and θ_2, albeit small, are of magnitudes larger than in the TwC-model.

Note that in all examples in Table 2, there exist principal angles of value 1.57. This can be explained as follows. In analogy to the smooth case Eq. (2) there are splittings

$$\begin{aligned}
\mathscr{H}_{h,N,\mathrm{co}} &:= \mathscr{H}_{h,N} \cap J\nabla\mathscr{F} \\
\mathscr{H}_{h,N,\partial\mathrm{ex}} &:= (\mathscr{H}_{h,N,\mathrm{co}})^{\perp} \cap \mathscr{H}_{h,N} \\
\mathscr{H}_{h,D,\mathrm{ex}} &:= \mathscr{H}_{h,D} \cap \nabla\mathscr{L} \\
\mathscr{H}_{h,D,\partial\mathrm{co}} &:= (\mathscr{H}_{h,D,\mathrm{ex}})^{\perp} \cap \mathscr{H}_{h,D}
\end{aligned}$$

of *discrete coexact Neumann fields*, *discrete boundary-exact Neumann fields* and so on, and it holds $\mathscr{H}_{h,N,\mathrm{co}} \perp \mathscr{H}_{h,D}$ and $\mathscr{H}_{h,D,\mathrm{ex}} \perp \mathscr{H}_{h,N}$ [12, Section 3.4]. Furthermore, if M_h is of type $\Sigma_{g,m}$ with $m \geq 1$, then we have [12, Lemmas 3.8/3.9]

$$\dim \mathscr{H}_{h,N,\mathrm{co}} = \mathscr{H}_{h,D,\mathrm{ex}} = m - 1.$$

This explains the $(m-1)$-many right angles in each of the experiments in Table 2.

Finally, it should be noted that there is a subtlety in the discrete theory that may arise in pathological examples and depends only on the grid combinatorics, i.e. the connectivity on the triangulation: whereas in the smooth case it is always $\mathscr{H}^k_N \cap \mathscr{H}^k_D = \{0\}$ [15, Thm. 3.4.4], the corresponding intersection of discrete spaces $\mathscr{H}_{h,N} \cap \mathscr{H}_{h,D}$ need not be trivial, resulting in invalid duality angles of value zero. This may happen if the discretization of the boundary is too low in comparison to the topological complexity (i.e. the numbers m and g of $\Sigma_{g,m}$) of the surface, or if there are very coarsely triangulated regions that form the only connections of the boundaries to the rest of the surface. A precise treatment as well as a criterion that guarantees the validity of the statement $\mathscr{H}_{h,N} \cap \mathscr{H}_{h,D} = \{0\}$ is given in [11, Section 3.4]. While it is important to keep this in mind, most models that arise in practice are not affected by this pathology.

Numerical Computation of Poincaré Duality Angles The numerical computation of principal angles between subspaces of a vector space is classical [4] and can be easily computed by means of the singular value decomposition (SVD). To this end we first compute orthonormal bases (ONB) $\mathscr{B}_N$ and $\mathscr{B}_D$ for the subspaces

$\mathscr{H}_{h,N}$ and $\mathscr{H}_{h,D}$, respectively. We refer the reader to [12, Sec. 4.1] for details on how to obtain these bases. By [4, Thm. 1] the principal angles are then the inverse cosines of the singular values of the matrix $\left(\langle u, v\rangle_{L^2}\right)_{u\in\mathscr{B}_N, v\in\mathscr{B}_D}$, which is of dimension $(2g+m-1)\times(2g+m-1)$. As $2g+m-1$ is typically small, the computation of this SVD poses no problems in terms of memory consumption or computation time. Listing 1 summarizes this procedure.

Listing 1 Numerical computation of discrete Poincaré duality angles

Input: Simplicial surface mesh M_h
  Compute ONB $\mathscr{B}_N$ for $\mathscr{H}_{h,N}$
  Compute ONB $\mathscr{B}_D$ for $\mathscr{H}_{h,D}$
  Assemble the matrix $M := \left(\langle u, v\rangle_{L^2}\right)_{u\in\mathscr{B}_N, v\in\mathscr{B}_D}$
  Compute the SVD $M = Y\cdot\Sigma\cdot Z^t$ with $\Sigma = \operatorname{diag}(\zeta_1,\ldots,\zeta_{2g+m-1})$, $\zeta_i \geq \zeta_{i+1}$
  return $\{\theta_i := \arccos\zeta_i\}_{i=1,\ldots,2g+m-1}$

5 Conclusion and Outlook

We have introduced the notion of *discrete Poincaré duality angles* on simplicial surfaces with boundary as an intrinsic quantity that sets the geometry, i.e. the metric properties of the surface, in relation to its topology, which is determined by its boundary components and the genus of the corresponding closed surface. In particular, these angles measure the influence of the boundary components on the overall geometry and quantify how far the surface is from being a closed surface. Rephrasing this fact algebraically, they quantify how far the two discrete Hodge-Morrey-Friedrichs decompositions Eqs. (4) and (5) differ from either the single decomposition Eq. (3) on closed surfaces of type $\Sigma_{g,0}$ or the complete orthogonal decomposition Eq. (6) on surfaces of type $\Sigma_{0,m}$ in which both the spaces $\mathscr{H}_{h,N}$ and $\mathscr{H}_{h,D}$ appear simultaneously as orthogonal subspaces. In this sense, the vector $(\theta_1,\ldots,\theta_{2g+m-1})$ of discrete Poincaré duality angles can be considered as a new intrinsic shape signature for a geometric-topological classification of simplicial surfaces with boundary.

On the other hand, it is still not clear in which way *precisely* the angles between Dirichlet and Neumann fields are related to the boundary components of M_h. The examples explicitly computed in [16] are a first starting point for the search of a relation that could be even quantitatively described, but as mentioned in [17], in general they still seem to be poorly understood. In this respect, the numerical computation of discrete Poincaré duality angles complements the smooth theory and may provide further insights. Moreover, for arbitrarily complex surfaces that arise from CAD-modelling or 3D scanning, an analytic computation seems out of reach.

Therefore, a better understanding of this correlation is very promising with regard to applications including metric-topological shape classification, extraction of certain vector field components with controlled characteristics and parametrization tasks of surfaces with boundary, and remains for future work.

Acknowledgments The authors thank the anonymous reviewers for their detailed and valuable feedback. This work was supported by the Einstein Center for Mathematics Berlin. The Laurent's hand model on which the hand model in Fig. 2 is based on is provided courtesy of INRIA by the AIM@SHAPE-VISIONAIR Shape Repository.

References

1. Arnold, D.N., Falk, R.S.: A uniformly accurate finite element method for the Reissner–Mindlin plate. SIAM J. Numer. Anal. **26**(6), 1276–1290 (1989)
2. Arnold, D.N., Falk, R.S., Winther, R.: Finite element exterior calculus, homological techniques, and applications. Acta Numer. **15**, 1–155 (2006)
3. Bhatia, H., Norgard, G., Pascucci, V., Bremer, P.-T.: The Helmholtz-Hodge decomposition - a survey. IEEE Trans. Vis. Comput. Graph. **19**(8), 1386–1404 (2013)
4. Björck, Å., Golub, G.H.: Numerical methods for computing angles between linear subspaces. Math. Comput. **27**(123), 579–594 (1973)
5. Bredon, G.E.: Topology and Geometry. Graduate Texts in Mathematics. Springer, New York (1993)
6. Dong, S., Kircher, S., Garland, M.: Harmonic functions for quadrilateral remeshing of arbitrary manifolds. Comput. Aided Geom. Des. **22**(5), 392–423 (2005)
7. Hirani, A.N.: Discrete exterior calculus. PhD thesis, California Institute of Technology (2003)
8. Kälberer, F., Nieser, M., Polthier, K.: QuadCover – surface parameterization using branched coverings. Comput. Graph. Forum **26**(3), 375–384 (2007)
9. Lee, J.M.: Introduction to Smooth Manifolds. Graduate Texts in Mathematics. Springer, New York (2003)
10. Munkres, J.R.: Elements of algebraic topology. Advanced Book Classics. Perseus Books, Cambridge, MA (1984)
11. Poelke, K.: Hodge-Type Decompositions for Piecewise Constant Vector Fields on Simplicial Surfaces and Solids with Boundary. PhD thesis, Freie Universität Berlin (2017)
12. Poelke, K., Polthier, K.: Boundary-aware Hodge decompositions for piecewise constant vector fields. Comput.-Aided Des. **78**, 126–136 (2016)
13. Polthier, K., Preuss, E.: Identifying vector field singularities using a discrete Hodge decomposition. In: Hege, H.-C., Polthier, K. (eds.) Visualization and Mathematics III, pp. 113–134. Springer, New York (2003)
14. Schall, O., Zayer, R., Seidel, H.-P.: Controlled field generation for quad-remeshing. In: Proceedings of the 2008 ACM Symposium on Solid and Physical Modeling, SPM '08, pp. 295–300. ACM, New York (2008)
15. Schwarz, G.: Hodge Decomposition: A Method for Solving Boundary Value Problems. Lecture Notes in Mathematics. Springer, Berlin, Heidelberg (1995)
16. Shonkwiler, C.: Poincaré Duality Angles on Riemannian Manifolds with Boundary. PhD thesis, University of Pennsylvania (2009)
17. Shonkwiler, C.: Poincaré duality angles and the Dirichlet-to-Neumann operator. Inverse Prob. **29**(4), 045007 (2013)
18. von Helmholtz, H.: Über Integrale der hydrodynamischen Gleichungen, welche den Wirbelbewegungen entsprechen. Journal für die reine und angewandte Mathematik **55**, 25–55 (1858)
19. Wardetzky, M.: Discrete Differential Operators on Polyhedral Surfaces - Convergence and Approximation. PhD thesis, Freie Universität Berlin (2006)
20. Xu, K., Zhang, H., Cohen-Or, D., Xiong, Y.: Dynamic harmonic fields for surface processing. Comput. Graph. **33**(3), 391–398 (2009)